PHYSICAL REVIEW C **93**, 051302(R) (2016)

Algebraic benchmark for prolate-oblate coexistence in nuclei

A. Leviatan and D. Shapira
Racah Institute of Physics, The Hebrew University, Jerusalem 91904, Israel
(Received 31 March 2016; published 19 May 2016)

We present a symmetry-based approach for prolate-oblate and spherical-prolate-oblate shape coexistence, in the framework of the interacting boson model of nuclei. The proposed Hamiltonian conserves the SU(3) and $\overline{\mathrm{SU(3)}}$ symmetry for the prolate and oblate ground bands and the U(5) symmetry for selected spherical states. Analytic expressions for quadrupole moments and $E2$ rates involving these states are derived and isomeric states are identified by means of selection rules.

DOI: 10.1103/PhysRevC.93.051302

A prominent feature in atomic nuclei, exemplifying a quantal mesoscopic system, is their ability to accommodate distinct shapes in their low-lying spectrum. Such shape coexistence in the same nucleus is known to occur widely across the nuclear chart [1,2]. The increased availability of rare isotope beams and advancement in high-resolution spectroscopy open new capabilities to investigate such phenomena in nuclei far from stability [3]. Notable empirical examples include the coexistence of prolate and oblate shapes in the neutron-deficient Kr [4], Se [5], and Hg [6] isotopes and the triple coexistence of spherical, prolate, and oblate shapes in ^{186}Pb [7]. A detailed microscopic interpretation of nuclear shape coexistence is a formidable task. In a shell model description of nuclei near shell closure, it is attributed to the occurrence of multiparticle-multihole intruder excitations. For medium-heavy nuclei, this necessitates drastic truncations of large model spaces, e.g., by Monte Carlo sampling [8,9] or by a bosonic approximation of nucleon pairs [10–16]. In a mean-field approach, based on energy density functionals, the coexisting shapes are associated with different minima of an energy surface calculated self-consistently. A detailed comparison with spectroscopic observables requires beyond mean-field methods, including restoration of broken symmetries and configuration mixing of angular-momentum and particle-number projected states [17,18]. Such extensions present a major computational effort and often require simplifying assumptions such as axial symmetry and/or a mapping to collective model Hamiltonians [14–19].

A recent global mean-field calculation of nuclear shape isomers identified experimentally accessible regions of nuclei with multiple minima in their potential-energy surface [20,21]. Such heavy-mass nuclei awaiting exploration are beyond the reach of realistic large-scale shell model calculations. With that in mind, we present a simple alternative to describe coexistence of prolate and oblate shapes in large deformed nuclei, away from shell closure, in the framework of the interacting boson model (IBM) [22]. The proposed approach emphasizes the role of remaining underlying symmetries, which provide physical insight and make the problem tractable.

The IBM has been widely used to describe quadrupole collective states in nuclei in terms of N monopole ($s^\dagger$) and quadrupole ($d^\dagger$) bosons, representing valence nucleon pairs. The model has U(6) as a spectrum-generating algebra and exhibits several dynamical symmetries (DSs) associated with chains of nested subalgebras. These solvable limits admit analytic solutions, with closed expressions for observables, quantum numbers, and definite selection rules. The DS chains with leading subalgebras U(5), SU(3), $\overline{\mathrm{SU(3)}}$, and SO(6) correspond to known paradigms of nuclear collective structure: spherical vibrator and prolate-, oblate-, and γ-soft deformed rotors, respectively. This identification is consistent with the geometric visualization of the model, obtained by an energy surface, $E_N(\beta,\gamma)$, defined by the expectation value of the Hamiltonian in the coherent (intrinsic) state [23,24],

$$|\beta,\gamma;N\rangle = (N!)^{-1/2}(b_c^\dagger)^N\,|0\rangle, \tag{1}$$

where $b_c^\dagger \propto \beta\cos\gamma d_0^\dagger + \beta\sin\gamma(d_2^\dagger + d_{-2}^\dagger)/\sqrt{2} + s^\dagger$. Here (β,γ) are quadrupole shape parameters whose values at the global minimum of $E_N(\beta,\gamma)$ define the equilibrium shape for a given Hamiltonian. The shape can be spherical ($\beta=0$) or deformed ($\beta>0$) with $\gamma=0$ (prolate), $\gamma=\pi/3$ (oblate), $0<\gamma<\pi/3$ (triaxial), or γ independent. The standard DS Hamiltonians support a single minimum in their energy surface and hence serve as benchmarks for the dynamics of a single quadrupole shape. In the present Rapid Communication, we propose a novel algebraic benchmark for describing the coexistence of prolate-oblate (P-O) shapes with equal β deformations and triple coexistence of spherical-prolate-oblate (S-P-O) shapes. We focus on the dynamics in the vicinity of the critical point where the corresponding multiple minima are near degenerate.

The DS limits appropriate to prolate and oblate shapes correspond, respectively, to the chains [22]

$$\mathrm{U(6)} \supset \mathrm{SU(3)} \supset \mathrm{SO(3)} \qquad |N,(\lambda,\mu),K,L\rangle, \tag{2a}$$

$$\mathrm{U(6)} \supset \overline{\mathrm{SU(3)}} \supset \mathrm{SO(3)} \qquad |N,(\bar\lambda,\bar\mu),\bar K,L\rangle. \tag{2b}$$

The indicated basis states are specified by quantum numbers which are the labels of irreducible representations (irreps) of the algebras in each chain. For a given N, the allowed SU(3) [$\overline{\mathrm{SU(3)}}$] irreps are $(\lambda,\mu)=(2N-4k-6m,2k)$ [$(\bar\lambda,\bar\mu)=(2k,2N-4k-6m)$] with k,m non-negative integers. The multiplicity label K ($\bar K$) corresponds geometrically to the projection of the angular momentum (L) on the symmetry axis. The basis states are eigenstates of the Casimir operator $\hat C_2[SU(3)]$ or $\hat C_2[\overline{\mathrm{SU(3)}}]$, where $\hat C_2[SU(3)]=2Q^{(2)}\cdot Q^{(2)}+\frac{3}{4}L^{(1)}\cdot L^{(1)}$, $Q^{(2)}=d^\dagger s+s^\dagger\tilde d-\frac{1}{2}\sqrt{7}(d^\dagger\tilde d)^{(2)}$, $L^{(1)}=\sqrt{10}(d^\dagger\tilde d)^{(1)}$,

$\tilde{d}_\mu = (-1)^\mu d_{-\mu}$, and $\hat{C}_2[\overline{\mathrm{SU(3)}}]$ is obtained by replacing $Q^{(2)}$ by $\bar{Q}^{(2)} = d^\dagger s + s^\dagger \tilde{d} + \frac{1}{2}\sqrt{7}(d^\dagger \tilde{d})^{(2)}$. The generators of SU(3) and $\overline{\mathrm{SU(3)}}$, $Q^{(2)}$ and $\bar{Q}^{(2)}$, and corresponding basis states, are related by a change of phase $(s^\dagger, s) \to (-s^\dagger, -s)$, induced by the operator $\mathcal{R}_s = \exp(i\pi \hat{n}_s)$, with $\hat{n}_s = s^\dagger s$. The DS Hamiltonian involves a linear combination of the Casimir operators in a given chain. The spectrum resembles that of an axially deformed rotovibrator composed of SU(3) [or $\overline{\mathrm{SU(3)}}$] multiplets forming rotational bands, with $L(L+1)$ splitting generated by $\hat{C}_2[\mathrm{SO(3)}] = L^{(1)} \cdot L^{(1)}$. In the SU(3) [or $\overline{\mathrm{SU(3)}}$] DS limit, the lowest irrep $(2N,0)$ [or $(0,2N)$] contains the ground band $g(K=0)$ [or $g(\bar{K}=0)$] of a prolate (oblate) deformed nucleus. The first excited irrep $(2N-4,2)$ [or $(2,2N-4)$] contains both the $\beta(K=0)$ and $\gamma(K=2)$ [or $\beta(\bar{K}=0)$ and $\gamma(\bar{K}=2)$] bands. Henceforth, we denote such prolate and oblate bands by (g_1,β_1,γ_1) and (g_2,β_2,γ_2), respectively. Since $\mathcal{R}_s Q^{(2)} \mathcal{R}_s^{-1} = -\bar{Q}^{(2)}$, the SU(3) and $\overline{\mathrm{SU(3)}}$ DS spectra are identical and the quadrupole moments of corresponding states differ in sign.

The phase transition between prolate and oblate shapes has been previously studied by varying a control parameter in the IBM Hamiltonian [25,26]. The latter, however, consisted of one- and two-body terms and hence could not accommodate simultaneously two deformed minima. A solvable albeit schematic description of asymmetric P-O shapes was analyzed in Ref. [27], with higher-order SU(3)-invariant IBM interactions. P-O coexistence was considered within the IBM with configuration mixing, by using different Hamiltonians for the normal and intruder configurations and a number-nonconserving mixing term [10–12]. In the present work, we adapt a different strategy. We construct a single number-conserving Hamiltonian which retains the virtues of SU(3) and $\overline{\mathrm{SU(3)}}$ DSs for the prolate and oblate ground bands and the U(5) DS for selected spherical states. The construction is based on an intrinsic-collective resolution of the Hamiltonian [28–30], a procedure used formerly in the study of spherical-deformed shape coexistence [31–33].

The intrinsic part of the critical-point Hamiltonian is required to satisfy

$$\hat{H}|N,(\lambda,\mu) = (2N,0),\ K=0,\ L\rangle = 0, \tag{3a}$$

$$\hat{H}|N,(\bar{\lambda},\bar{\mu}) = (0,2N),\ \bar{K}=0,\ L\rangle = 0. \tag{3b}$$

Equivalently, $\hat{H}$ annihilates the intrinsic states of Eq. (1), with $(\beta=\sqrt{2},\gamma=0)$ and $(\beta=-\sqrt{2},\gamma=0)$, which are the lowest- and highest-weight vectors in the irreps $(2N,0)$ and $(0,2N)$ of SU(3) and $\overline{\mathrm{SU(3)}}$, respectively. The resulting Hamiltonian is found to be

$$\hat{H} = h_0\, P_0^\dagger \hat{n}_s P_0 + h_2\, P_0^\dagger \hat{n}_d P_0 + \eta_3\, G_3^\dagger \cdot \tilde{G}_3, \tag{4}$$

where $P_0^\dagger = d^\dagger \cdot d^\dagger - 2(s^\dagger)^2$, $G_{3,\mu}^\dagger = \sqrt{7}[(d^\dagger d^\dagger)^{(2)} d^\dagger]_\mu^{(3)}$, $\tilde{G}_{3,\mu} = (-1)^\mu G_{3,-\mu}$, $\hat{n}_d = \sum_\mu d_\mu^\dagger d_\mu$ and the centered dot denotes a scalar product. The corresponding energy surface, $E_N(\beta,\gamma) = N(N-1)(N-2)\tilde{E}(\beta,\gamma)$, is given by

$$\tilde{E}(\beta,\gamma) = \{(\beta^2-2)^2[h_0 + h_2\beta^2] + \eta_3\beta^6 \sin^2(3\gamma)\} \times (1+\beta^2)^{-3}. \tag{5}$$

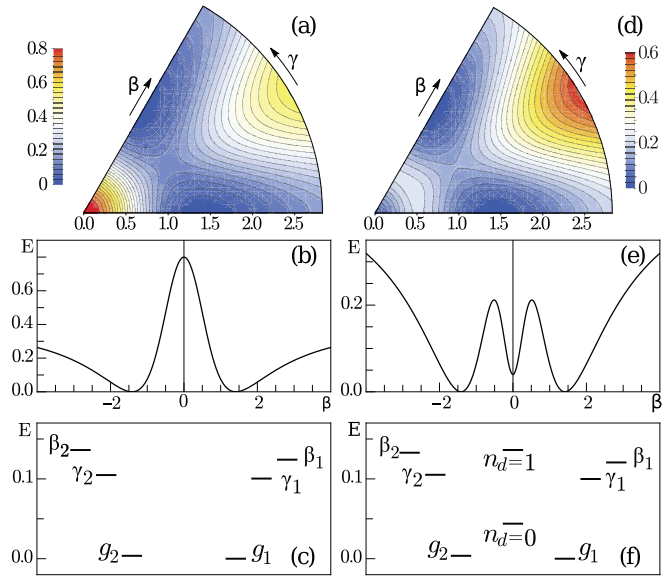

FIG. 1. Contour plots of the energy surface (5) [top row], $\gamma = 0$ sections [middle row], and band-head spectrum [bottom row] for the Hamiltonian (9), with $\alpha = 0.018$, $\eta_3 = 0.571$, $\rho = 0$, $N = 20$. Panels (a), (b), and (c) [(d), (e), and (f)] correspond to the choice $h_0 = 0.2$, $h_2 = 0.4$ [$h_0 = 0.01$, $h_2 = 0.5$], resulting in prolate-oblate [spherical-prolate-oblate] shape coexistence.

The surface is an even function of β and $\Gamma = \cos 3\gamma$, and can be transcribed as $\tilde{E}(\beta,\gamma) = z_0 + (1+\beta^2)^{-3}[A\beta^6 + B\beta^6\Gamma^2 + D\beta^4 + F\beta^2]$, with $A = -4h_0 + h_2 + \eta_3$, $B = -\eta_3$, $D = -(11h_0 + 4h_2)$, $F = 4(h_2 - 4h_0)$, $z_0 = 4h_0$. It is the most general form of a surface accommodating degenerate prolate and oblate extrema with equal β deformations, for an Hamiltonian with cubic terms [34,35]. For $h_0, h_2, \eta_3 \geqslant 0$, $\hat{H}$ is positive definite and $\tilde{E}(\beta,\gamma)$ has two degenerate global minima, $(\beta = \sqrt{2}, \gamma = 0)$ and $(\beta = \sqrt{2}, \gamma = \pi/3)$ [or equivalently $(\beta = -\sqrt{2}, \gamma = 0)$], at $\tilde{E} = 0$. $\beta = 0$ is always an extremum, which is a local minimum (maximum) for $F > 0$ ($F < 0$), at $\tilde{E} = 4h_0$. Additional extremal points include (i) a saddle point: $[\beta_*^2 = \frac{2(4h_0 - h_2)}{h_0 - 7h_2}, \gamma = 0, \pi/3]$, at $\tilde{E} = \frac{4(h_0+2h_2)^3}{81(h_0-h_2)^2}$, and (ii) a local maximum and a saddle point: $[\beta_{**}^2, \gamma = \pi/6]$, at $\tilde{E} = \frac{1}{3}(1+\beta_{**}^2)^{-2}\beta_{**}^2[D\beta_{**}^2 + 2F] + z_0$, where β_{**}^2 is a solution of $(D-3A)\beta_{**}^4 + 2(F-D)\beta_{**}^2 - F = 0$. The saddle points, when they exist, support a barrier separating the various minima, as seen in Fig. 1.

The members of the prolate and oblate ground bands, Eq. (3), are zero-energy eigenstates of $\hat{H}$ (4), with good SU(3) and $\overline{\mathrm{SU(3)}}$ symmetry, respectively. For large N, the spectrum is harmonic, involving β and γ vibrations about the respective deformed minima, with frequencies

$$\epsilon_{\beta 1} = \epsilon_{\beta 2} = \tfrac{8}{3}(h_0 + 2h_2)N^2, \tag{6a}$$

$$\epsilon_{\gamma 1} = \epsilon_{\gamma 2} = 4\eta_3 N^2. \tag{6b}$$

For $h_0 = 0$, also $\beta = 0$ becomes a global minimum at $\tilde{E} = 0$, resulting in three degenerate minima, corresponding to triple coexistence of prolate, oblate, and spherical shapes. $\hat{H}(h_0 = 0)$

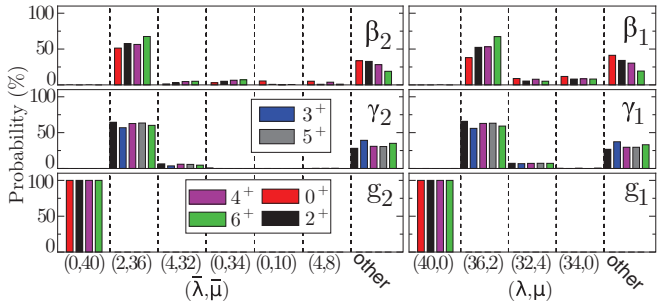

FIG. 2. SU(3) (λ,μ) and $\overline{\text{SU(3)}}$ $(\bar{\lambda},\bar{\mu})$ decomposition for members of the prolate (g_1,β_1,γ_1) and oblate (g_2,β_2,γ_2) bands, eigenstates of $\hat{H}'$ (9) with parameters as in Fig. 1(c), resulting in prolate-oblate shape coexistence. The column "other" depicts a sum of probabilities, each less than 0.5%.

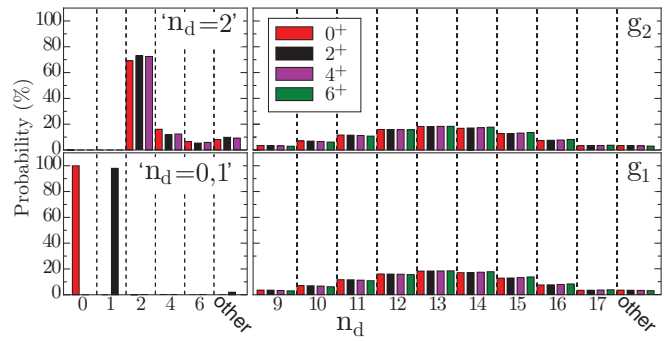

FIG. 3. U(5) n_d decomposition for spherical states (left panels) and for members of the g_1 and g_2 bands (right panels), eigenstates of $\hat{H}'$ (9) with parameters as in Fig. 1(f), resulting in spherical-prolate-oblate shape coexistence.

has the following U(5) basis state:

$$\hat{H}(h_0=0)|N,n_d=\tau=L=0\rangle=0, \tag{7}$$

as an eigenstate. Equivalently, it annihilates the intrinsic state of Eq. (1), with $\beta=0$. The additional normal modes involve quadrupole vibrations about the spherical minimum, with frequency

$$\epsilon=4h_2N^2. \tag{8}$$

When $\beta=0$ is only a local minimum, the $(n_d=L=0)$ state experiences a shift of order $4h_0N^3$.

The Hamiltonian of Eq. (4) is invariant under a change of sign of the s bosons and hence commutes with the $\mathcal{R}_s$ operator mentioned above. Consequently, all nondegenerate eigenstates of $\hat{H}$ have well-defined s parity. This implies vanishing quadrupole moments for an $E2$ operator, which is odd under such sign change. To overcome this difficulty, we introduce a small s-parity-breaking term, $\alpha\hat{\theta}_2=\alpha[-\hat{C}_2[SU(3)]+2\hat{N}(2\hat{N}+3)]$, which contributes to $\tilde{E}(\beta,\gamma)$, $\tilde{\alpha}(1+\beta^2)^{-2}[(\beta^2-2)^2+2\beta^2(2-2\sqrt{2}\beta\Gamma+\beta^2)]$, with $\tilde{\alpha}=\alpha/(N-2)$. The linear Γ dependence distinguishes the two deformed minima and slightly lifts their degeneracy, as well as that of the normal modes (6). Replacing $\hat{\theta}_2$ by $\bar{\theta}_2$, associated with $\hat{C}_2[\overline{\text{SU(3)}}]$, leads to similar effects but interchanges the role of prolate and oblate bands. Identifying the collective part with $\hat{C}_2[\text{SO(3)}]$, we arrive at the following complete Hamiltonian:

$$\hat{H}'=\hat{H}(h_0,h_2,\eta_3)+\alpha\,\hat{\theta}_2+\rho\,\hat{C}_2[\text{SO(3)}], \tag{9}$$

where $\hat{H}(h_0,h_2,\eta_3)$ is the Hamiltonian of Eq. (4).

Figures 1(a)-1(b)-1(c) [1(d)-1(e)-1(f)] show $\tilde{E}(\beta,\gamma)$, $\tilde{E}(\beta,\gamma=0)$ and the bandhead spectrum of $\hat{H}'$ (9), with parameters ensuring P-O [S-P-O] minima. The prolate g_1 band remains solvable with energy $E_{g1}(L)=\rho L(L+1)$. The oblate g_2 band experiences a slight shift of order $\frac{32}{9}\alpha N^2$ and displays a rigid-rotor-like spectrum. In the case of P-O coexistence, the SU(3) and $\overline{\text{SU(3)}}$ decomposition in Fig. 2 demonstrates that these bands are pure DS basis states, with $(2N,0)$ and $(0,2N)$ characters, respectively, while excited β and γ bands exhibit considerable mixing. In the case of triple S-P-O coexistence, the prolate and oblate bands show similar behavior. A new aspect is the simultaneous occurrence in the spectrum [Fig. 1(f)] of spherical type of states, whose wave functions are dominated by a single n_d component. As shown in Fig. 3, the lowest spherical states have quantum numbers $(n_d=L=0)$ and $(n_d=1,L=2)$, and hence coincide with pure U(5) basis states, while higher spherical states have a pronounced $(\sim 70\%)$ $n_d=2$ component. This structure should be contrasted with the U(5) decomposition of deformed states (belonging to the g_1 and g_2 bands) which, as shown in Fig. 3, have a broad n_d distribution. The purity of selected sets of states with respect to SU(3), $\overline{\text{SU(3)}}$, and U(5), in the presence of other mixed states, are the hallmarks of a partial dynamical symmetry [36,37]. It is remarkable that a simple Hamiltonian, as in Eq. (9), can accommodate simultaneously several incompatible symmetries in a segment of the spectrum.

Since the wave functions for the members of the g_1 and g_2 bands are known, one can derive analytic expressions for their quadrupole moments and $E2$ transition rates. Considering the $E2$ operator

$$T(E2)=e_B(d^\dagger s+s^\dagger\tilde{d}), \tag{10}$$

with an effective charge e_B, the quadrupole moments are found to have equal magnitudes and opposite signs,

$$Q_L=\mp e_B\sqrt{\frac{16\pi}{40}}\frac{L}{2L+3}\frac{4(2N-L)(2N+L+1)}{3(2N-1)}, \tag{11}$$

where the minus (plus) sign corresponds to the prolate-g_1 (oblate-g_2) band. The $B(E2)$ values for intraband $(g_1\to g_1$, $g_2\to g_2)$ transitions,

$$B(E2;g_i,L+2\to g_i,L)=e_B^2\frac{3(L+1)(L+2)}{2(2L+3)(2L+5)}\frac{(4N-1)^2(2N-L)(2N+L+3)}{18(2N-1)^2}, \tag{12}$$

are the same. These properties are ensured by the fact that $\mathcal{R}_sT(E2)\mathcal{R}_s^{-1}=-T(E2)$. Interband $(g_2\leftrightarrow g_1)$ $E2$ transitions, are extremely weak. This follows from the fact that the L states of the g_1 and g_2 bands exhaust, respectively, the $(2N,0)$ and $(0,2N)$ irrep of SU(3) and $\overline{\text{SU(3)}}$. $T(E2)$ as a (2,2) tensor under both algebras can thus connect the $(2N,0)$ irrep of

g_1 only with the $(2N-4,2)$ component in g_2, which, however, is vanishingly small. The selection rule $g_1 \nleftrightarrow g_2$ is valid also for a more general $E2$ operator, obtained by adding $Q^{(2)}$ or $\bar{Q}^{(2)}$ to the operator of Eq. (10) since the latter, as generators, cannot mix different irreps of SU(3) or $\overline{\mathrm{SU}(3)}$. By similar arguments, $E0$ transitions in between the g_1 and g_2 bands are extremely weak, since the relevant operator, $T(E0) \propto \hat{n}_d$, is a combination of (0,0) and (2,2) tensors under both algebras. Accordingly, the $L=0$ bandhead state of the higher (g_2) band cannot decay to the lower g_1 band and hence displays characteristic features of an isomeric state. In contrast to g_1 and g_2, excited β and γ bands are mixed and hence are connected by $E2$ transitions to these ground bands. Their quadrupole moments are found numerically to resemble, for large N, the collective model expression $Q(K,L) = \frac{3K^2-L(L+1)}{(L+1)(2L+3)} q_K$, with $q_K > 0$ ($q_K < 0$) for prolate (oblate) bands.

In the case of triple (S-P-O) coexistence, since $T(E2)$ obeys the selection rule $\Delta n_d = \pm 1$, the spherical states, $(n_d = L = 0)$ and $(n_d = 1, L = 2)$, have no quadrupole moment and the $B(E2)$ value for their connecting transition, obeys the U(5)-DS expression [22]

$$B(E2; n_d = 1, L = 2 \rightarrow n_d = 0, L = 0) = e_B^2 N. \qquad (13)$$

These spherical states have very weak $E2$ transitions to the deformed ground bands, because they exhaust the $(n_d = 0,1)$ irreps of U(5), and the $n_d = 2$ component in the $(L = 0,2,4)$ states of the g_1 and g_2 bands is extremely small, of order $N^3 3^{-N}$. There are also no $E0$ transitions involving these spherical states, since $T(E0)$ is diagonal in n_d. The lowest $(n_d = L = 0)$ state has, therefore, the attributes of a spherical isomer state. The analytic expressions of Eqs. (11)–(13) are parameter-free predictions, except for a scale, and can be used to compare with measured values of these observables and to test the underlying SU(3), $\overline{\mathrm{SU}(3)}$, and U(5) partial symmetries.

The proposed Hamiltonian (9) involves three-body interactions. Similar cubic terms were encountered in previous studies within the IBM, in conjunction with triaxiality [38,39], band anharmonicity [40,41], and signature splitting [42,43] in deformed nuclei. Higher-order terms show up naturally in microscopic-inspired IBM Hamiltonians derived by a mapping from self-consistent mean-field calculations [15,44]. Near shell closure $\hat{H}'$ (9) can be regarded as an effective number-conserving Hamiltonian, which simulates the excluded intruder configurations by means of higher-order terms. Indeed, the energy surfaces of the IBM with configuration mixing [11,12,45] contain higher powers of β^2 and $\beta^3 \cos 3\gamma$, as in Eq. (5). Recalling the microscopic interpretation of the IBM bosons as images of identical valence-nucleon pairs, the results of the present study suggest that for nuclei far from shell closure, shape coexistence can occur within the same valence space.

As discussed, the coexisting prolate and oblate ground bands of $\hat{H}'$ (9) are unmixed and retain their individual SU(3) and $\overline{\mathrm{SU}(3)}$ characters. This situation is different from that encountered in the neutron-deficient Kr [4] and Hg [6] isotopes, where the observed structures are strongly mixed. It is in line with the recent evidence for shape coexistence in neutron-rich Sr isotopes, where spherical and prolate-deformed configurations exhibit very weak mixing [46]. Band mixing can be incorporated in the present formalism by adding kinetic rotational terms which do not affect the shape of the energy surface [28–30,35] but may destroy the partial symmetry property of the states. The evolution of structure away from the critical point can be studied by varying the coupling constant α in Eq. (9). Larger values of α will shift the energy of the nonyrast ground band (the oblate g_2 band in the example considered). In the case of a triple S-P-O coexistence, adding an $\hat{n}_d$ term to $\hat{H}(\eta_0 = 0)$ will leave the $n_d = 0$ spherical ground state unchanged but will shift the prolate and oblate bands to higher energy. The same method of intrinsic-collective resolution can be used to identify appropriate Hamiltonians for an asymmetric prolate-oblate coexistence with different β deformations. Details of such extensions and refinements will be reported elsewhere.

In summary, we have presented a number-conserving rotational-invariant Hamiltonian which captures essential features of P-O and S-P-O coexistence in nuclei. It preserves particular symmetries for certain prolate and oblate bands and spherical states, with closed expressions for $E2$ moments and transition rates, which are the observables most closely related to the nuclear shape. These attributes turn the proposed framework into a suitable algebraic benchmark for the study of shape coexistence in nuclei, providing a convenient starting point, guidance, and test ground for more detailed treatments of this intriguing phenomena.

This research was supported by the Israel Science Foundation (Grant No. 493/12).

[1] K. Heyde and J. L. Wood, Rev. Mod. Phys. **83**, 1467 (2011).
[2] Edited by J. L. Wood and K. Heyde, *Focus Review on Shape Coexistence in Nuclei*, J. Phys. G **43**, 024001–024013 (2016).
[3] D. G. Jenkins, Nat. Phys. **10**, 909 (2014).
[4] E. Clément *et al.*, Phys. Rev. C **75**, 054313 (2007).
[5] J. Ljungvall *et al.*, Phys. Rev. Lett. **100**, 102502 (2008).
[6] N. Bree *et al.*, Phys. Rev. Lett. **112**, 162701 (2014).
[7] A. N. Andreyev *et al.*, Nature (London) **405**, 430 (2000).
[8] T. Mizusaki, T. Otsuka, Y. Utsuno, M. Honma, and T. Sebe, Phys. Rev. C **59**, R1846(R) (1999).
[9] Y. Tsunoda, T. Otsuka, N. Shimizu, M. Honma, and Y. Utsuno, Phys. Rev. C **89**, 031301(R) (2014).
[10] R. Fossion, K. Heyde, G. Thiamova, and P. Van Isacker, Phys. Rev. C **67**, 024306 (2003).
[11] A. Frank, P. Van Isacker, and C. E. Vargas, Phys. Rev. C **69**, 034323 (2004).
[12] I. O. Morales, A. Frank, C. E. Vargas, and P. Van Isacker, Phys. Rev. C **78**, 024303 (2008).
[13] J. E. García-Ramos and K. Heyde, Phys. Rev. C **89**, 014306 (2014).
[14] K. Nomura, R. Rodríguez-Guzmán, L. M. Robledo, and N. Shimizu, Phys. Rev. C **86**, 034322 (2012).
[15] K. Nomura, R. Rodríguez-Guzmán, and L. M. Robledo, Phys. Rev. C **87**, 064313 (2013).

[16] K. Nomura, T. Otsuka, and P. Van Isacker, J. Phys. G **43**, 024008 (2016).
[17] J. M. Yao, M. Bender, and P.-H. Heenen, Phys. Rev. C **87**, 034322 (2013).
[18] Z. P. Li, T. Nikšić, and D. Vretenar, J. Phys. G **43**, 024005 (2016).
[19] K. Nomura, T. Nikšić, T. Otsuka, N. Shimizu, and D. Vretenar, Phys. Rev. C **84**, 014302 (2011).
[20] P. Möller, A. J. Sierk, R. Bengtsson, H. Sagawa, and T. Ichikawa, Phys. Rev. Lett. **103**, 212501 (2009).
[21] P. Möller, A. J. Sierk, R. Bengtsson, H. Sagawa, and T. Ichikawa, At. Data Nucl. Data Tables **98**, 149 (2012).
[22] F. Iachello and A. Arima, *The Interacting Boson Model* (Cambridge University Press, Cambridge, UK, 1987).
[23] J. N. Ginocchio and M. W. Kirson, Phys. Rev. Lett. **44**, 1744 (1980).
[24] A. E. L. Dieperink, O. Scholten, and F. Iachello, Phys. Rev. Lett. **44**, 1747 (1980).
[25] J. Jolie, R. F. Casten, P. von Brentano, and V. Werner, Phys. Rev. Lett. **87**, 162501 (2001).
[26] J. Jolie and A. Linnemann, Phys. Rev. C **68**, 031301(R) (2003).
[27] Y. Zhang, F. Pan, Y. X. Liu, Y. A. Luo, and J. P. Draayer, Phys. Rev. C **85**, 064312 (2012).
[28] M. W. Kirson and A. Leviatan, Phys. Rev. Lett. **55**, 2846 (1985).
[29] A. Leviatan, Ann. Phys. (NY) **179**, 201 (1987).
[30] A. Leviatan and M. W. Kirson, Ann. Phys. (NY) **201**, 13 (1990).
[31] A. Leviatan, Phys. Rev. C **74**, 051301(R) (2006).
[32] A. Leviatan, Phys. Rev. Lett. **98**, 242502 (2007).
[33] M. Macek and A. Leviatan, Ann. Phys. (NY) **351**, 302 (2014).
[34] P. Van Isacker and J. Q. Chen, Phys. Rev. C **24**, 684 (1981).
[35] A. Leviatan and B. Shao, Phys. Lett. B **243**, 313 (1990).
[36] A. Leviatan, Phys. Rev. Lett. **77**, 818 (1996).
[37] A. Leviatan, Prog. Part. Nucl. Phys. **66**, 93 (2011).
[38] K. Heyde, P. Van Isacker, M. Waroquier, and J. Moreau, Phys. Rev. C **29**, 1420 (1984).
[39] N. V. Zamfir and R. F. Casten, Phys. Lett. B **260**, 265 (1991).
[40] J. E. García-Ramos, J. M. Arias, and P. Van Isacker, Phys. Rev. C **62**, 064309 (2000).
[41] J. E. García-Ramos, A. Leviatan, and P. Van Isacker, Phys. Rev. Lett. **102**, 112502 (2009).
[42] D. Bonatsos, Phys. Lett. B **200**, 1 (1988).
[43] A. Leviatan, J. E. García-Ramos, and P. Van Isacker, Phys. Rev. C **87**, 021302(R) (2013).
[44] K. Nomura, N. Shimizu, D. Vretenar, T. Nikšić, and T. Otsuka, Phys. Rev. Lett. **108**, 132501 (2012).
[45] V. Hellemans, P. Van Isacker, S. De Baerdemacker, and K. Heyde, Nucl. Phys. A **819**, 11 (2009).
[46] E. Clément *et al.*, Phys. Rev. Lett. **116**, 022701 (2016).